Electronic Supplementary Material (ESI) for Dalton Transactions.

Palladium nanoparticles confined in uncoordinated amine groups of metal-organic frameworks as efficient hydrogen evolution electrocatalysts

Huimin Liu[a], Chen Wang[a], Chang Liu[a], Xing Zong[b], Yongfei Wang[a,b]* , Zhizhi Hu[a], Zhiqiang Zhang[a]*

[a]School of Chemical Engineering, University of Science and Technology Liaoning 185 Qianshan Zhong Road, Anshan 114051, P. R. China

[b]School of Materials and Metallurgy, University of Science and Technology Liaoning Anshan, Liaoning 114051, P. R. China

E-mail: wyf8307@ustl.edu.cn, zzq@ustl.edu.cn

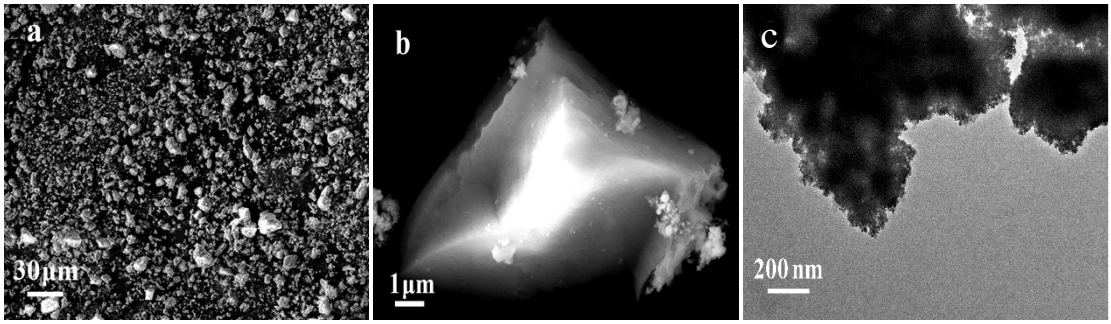

Figure S1. (a,b) SEM images of Uio-66-NH_2 and Pd@Uio-66, respectively. (c) HRTEM images of Pd@Uio-66-NH_2.

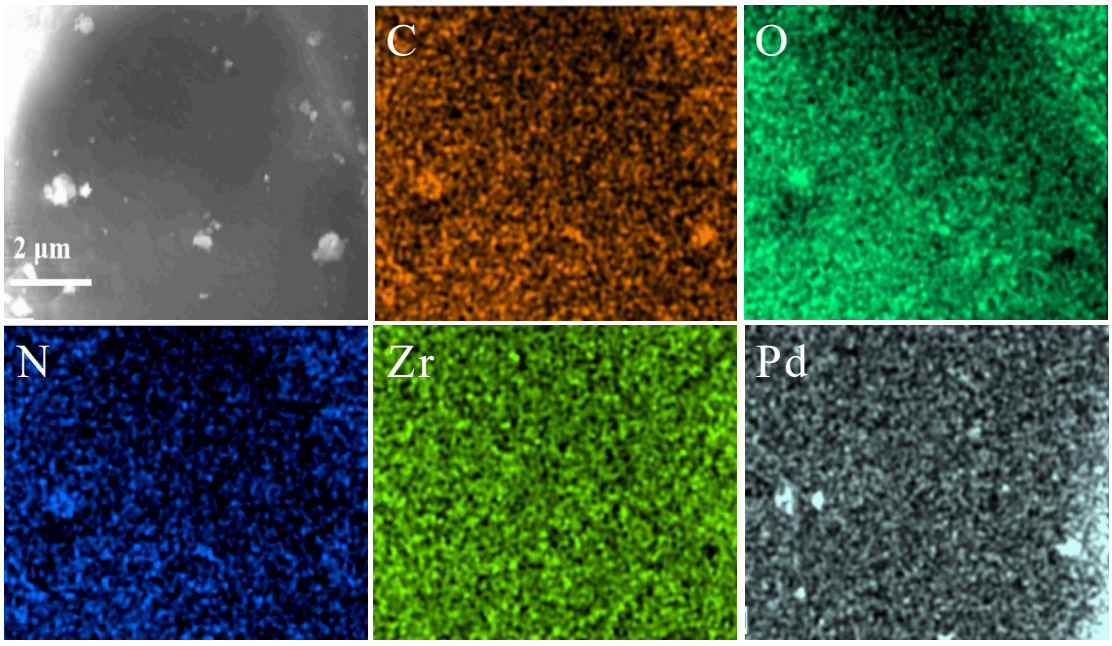

Figure S2. Elemental mappings of C, N, O, Zr, and Pd for Pd@UiO-66-NH_2.

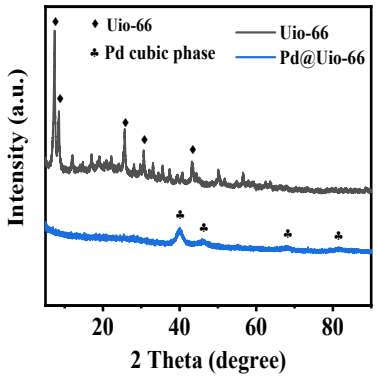

Figure S3. XRD image of Uio-66 and Pd@Uio-66.

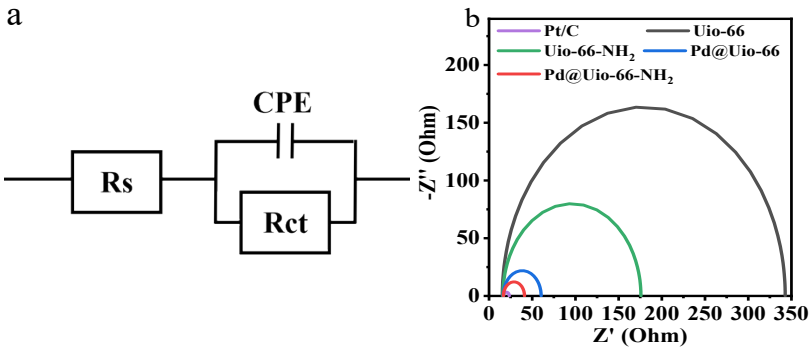

Figure S4. (a) The equivalent circuit used to simulate the Nyquist plots, where Rs represents the solution resistance, the Rct related to the charge transfer resistance at the interface between catalysts and the electrolyte and CPE reflects constant phase element. (b) Nyquist plots of the various electrocatalysts.

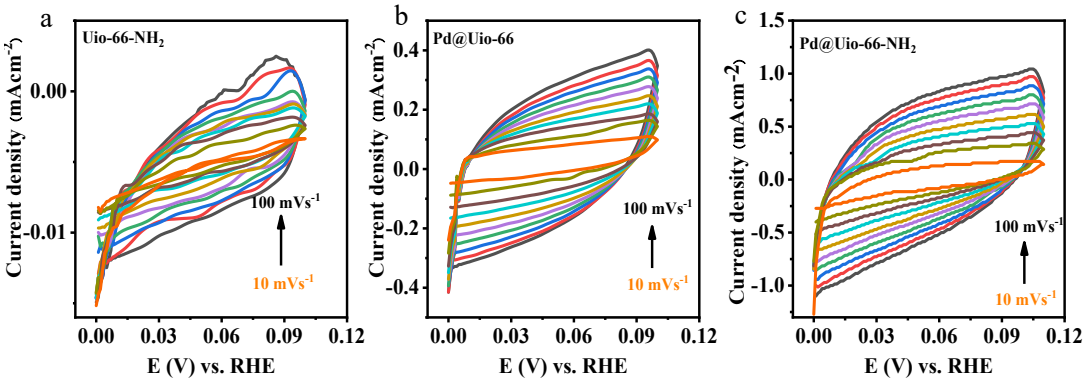

Figure S5. CV curves of (a) Uio-66-NH_2, (b) Pd@Uio-66 and (c) Pd@Uio-66-NH_2 at different scan rates.

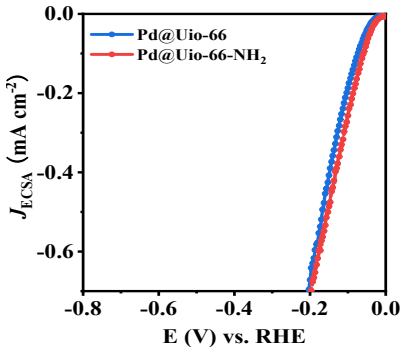

Figure S6. ECSA normalized LSV curves of Pd@Uio-66 and (c) Pd@Uio-66-NH_2.

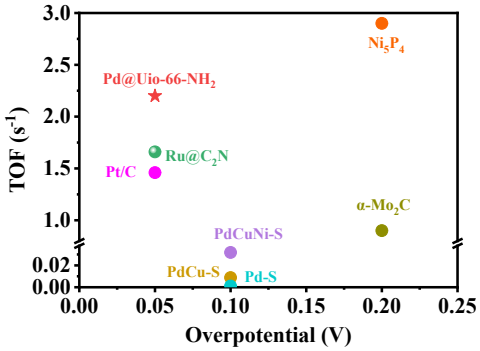

Figure S7. TOF values of Pd@Uio-66-NH_2 compared with the reported catalysts.

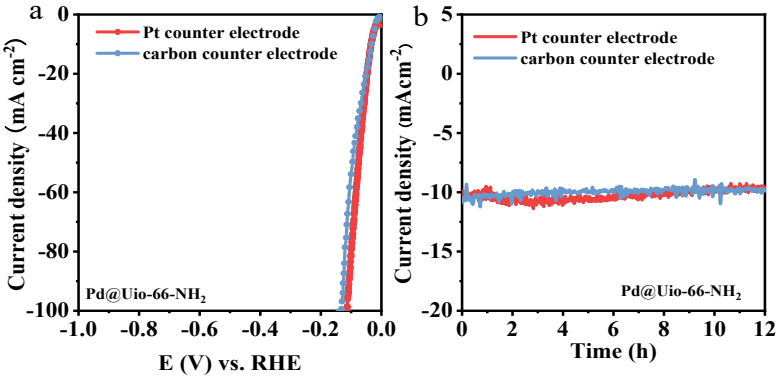

Figure S8. LSV curves (a) and the stability test (b) for Pd@Uio-66-NH_2 by using graphite electrode as the counter electrode.

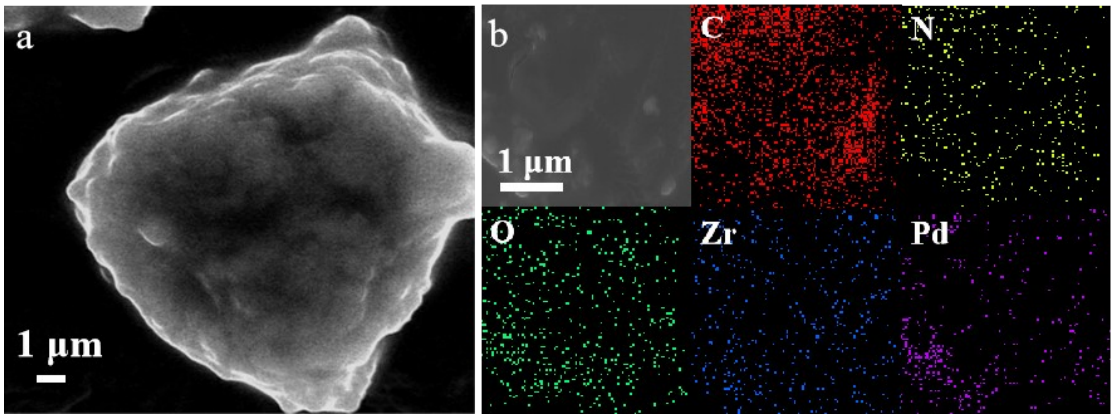

Figure S9. (a) SEM image and (b) corresponding elemental mappings of Pd@Uio-66-NH_2 after stability test.

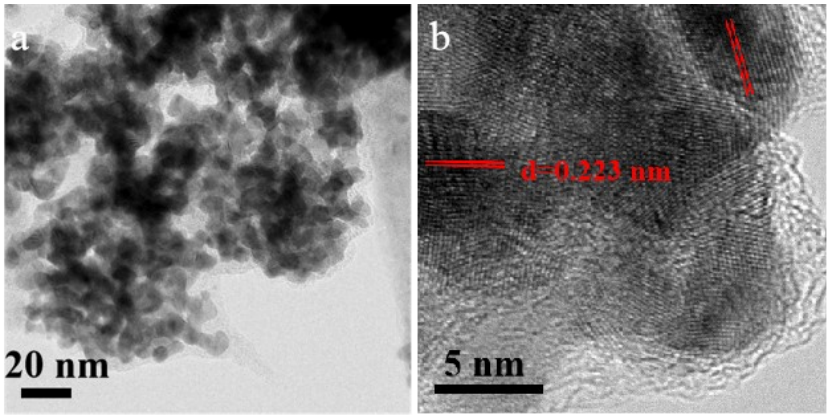

Figure S10. (a,b) HRTEM images of Pd@Uio-66-NH_2 after stability test.

Table S1. Comparison the HER activity of Pd@Uio-66-NH_2 with mentioned in this paper catalysts in 0.5 M H_2SO_4 solutions.

Catalyst	E_{onset} (mV)	E_{10} (mV)	E_{20} (mV)
Pt/C	19	28	35
Uio-66	152	403	476
Uio-66-NH_2	59	230	318
Pd@Uio-66	25	70	99
Pd@Uio-66-NH_2	22	34	47

Table S2. Comparison the HER activity of Pd@Uio-66-NH_2 with other Pd-based catalysts in 0.5 M H_2SO_4 solutions.

Catalyst	Overpotential @10 mA cm^{-2} (mV)	Tafel slope (mV dec^{-1})	Reference
Pd@Uio-66-NH_2	34	41	This work
Pd/MOF	~400	85	Mater. Chem. Phys. 2020, 254, 123481
Pd/HASG	63	42	Catal. Today. 2020, 357, 279
Pd1/NMC	37	37	Int. J. Hydrogen Energ. 2022, 47, 39319
PdC	96	82	ACS Appl. Energy Mater. 2021, 4, 575
PdSNC	30	56	ACS Appl. Energy Mater. 2021, 4, 575
Pd-TiO_2	108	64	Mater. Today Nano, 2019, 6, 10038
Pd/SW_2	130	82.4	J. Catal. 2019, 380, 215
Pd_4S-SNC	32	52	Small 2021, 17, 2007511
Cu-Pd/HASG	145	75	Catal. Today. 2020,357, 279
$PdSe_2$	150	70	Appl. Surf. Sci. 2021, 570, 151178
$Pd_{83.5}Ir_{16.5}$	73	43.6	Inorg. Chem. 2020, 59, 3321

Table S3. Comparison the TOF values of Pd@Uio-66-NH_2 with the reported catalysts in 0.5 M H_2SO_4 solutions.

Catalyst	TOF (s^{-1}) @ η (V)	Reference
Pd@Uio-66-NH_2	2.2@0.05	This work
Pt/C	1.46@0.05	Adv. Sci. 2021, 8, 2001881
Ru@C_2N	1.66@0.05	Nat. Nanotechnol. 2017, 12, 441
PdCuNi-S	0.03188@0.1	Appl. Catal. B-Environ. 2019, 246, 156
PdCu-S	0.0088@0.1	Appl. Catal. B-Environ. 2019, 246, 156
Pd-S	0.0011@0.1	Appl. Catal. B-Environ. 2019, 246, 156
Ni_5P_4	2.9@0.2	ACS Catal. 2013, 3, 166
α-Mo_2C	0.9@0.2	J. Mater. Chem. A 2015, 3, 8361